Anal. Chem. **1996,** *68,* 3359−3363

Laser Two-Photon Ionization of Pyrene on Contaminated Soils

Vladimir V. Gridin, Alona Korol, Valery Bulatov, and Israel Schechter*

Department of Chemistry, Technion-Israel Institute of Technology, Haifa 32000, Israel

We report a first attempt to use the laser multiphoton ionization method for analysis of trace aromatic compounds on the surface of environmental (soils) and artificial (silica) samples. The measurement setup is composed of a N_2 pulsed laser and a fast conductivity detection system. The technique has been tested for detection of pyrene deposited on moist fine-powdered samples. The observed photoionization signals have indicated a gradual increase in the photoionization current and charge as a function of increasing concentration of pyrene/hexane solutions used for sample contamination. Contaminants have been analyzed in several (organic and inorganic) environmental samples, and a method to compensate for matrix effects is suggested. A contamination model is assumed and applied in order to renormalize all signals and provide an useful calibration plot. This calibration plot provides an upper estimate of pyrene LOD as 35 ng/g.

Laser multiphoton ionization (MPI) has been recognized as a very sensitive method of analysis, with high selectivity in its resonant mode.[1−5] In this method a laser pulse is applied to ionize a substrate in a process that involves several photons. The MPI technique has been coupled to many ion detection systems: The most powerful tool is obtained with a full MS detection system;[6,7] however, this setup is rather complicated and expensive. Simple and low-cost detection systems have been also developed, suggesting a possible application to chemical sensors.[8−12] Recently, such a new detection system was been proposed for on-line analysis of aromatic compounds in ambient air.[13−16]

One of the simplest detection systems is the fast conductivity method, where the current due to the emitted electrons is monitored. This method has been successfully applied to a variety of systems of considerably analytical interest. Many such applications have been pioneered by Winefordner et al.[9] and by Ogawa et al.[10] These include trace organic compounds in nonpolar solvents,[17−26] on metal,[27−29] and on water surface.[30−31] Two-color MPI,[32−34] as well as single crystals[35] and aerosol particles,[36] have also been investigated. The detection limits of this technique, according to some of the recently reported studies, can be as low as sub-ppb or even ppt levels of trace contamination.[25,31]

There are numerous uses and needs for relatively low cost analytical techniques of this kind, especially when on-line and in situ abilities of the method are applied. One of the most important fields of application is concerned with the research directions found in environmental studies of atmospheric, water resources, and soil pollutants. To the best of our knowledge, this technique has not been reported in regard to the study of soil contamination. In this paper we report results of such an attempt and suggest further investigation possibilities that seem to be a natural extension of the findings reported herein. Our photoionization study of soil samples has been conducted under ambient laboratory conditions. The focus of this preliminary study is on testing the fast conductivity technique in terms of its detection ability of pyrene contamination deposited onto soil samples, where MPI is induced by a pulsed N_2 laser.

(1) Letokhov, V. S. *Laser Analytical Spectrochemistry*; Adam Hilger: Bristol, PA, 1986.
(2) Lambropoulos, P., Smith, S. J., Eds. *Multiphoton Ionization*; Proceedings of the 3rd International Conference, Iraklion, Crete, Greece, Sept 1984; Spring-Verlag: Berlin, 1984.
(3) *Laser Applications to Chemical Analysis*; 1990 Technical Digest Series; Optical Society of America: Washington, DC, 1990; Vol. 2.
(4) Ogawa, T. *Anal. Sci.* **1991**, *7*, 1475.
(5) Hurst, G. S.; Payne, M. G.; Kramer, S. D.; Young, J. P. *Rev. Mod. Phys.* **1979**, *51*, 767−819.
(6) Burlingame, A. L.; Millington, D. S.; Norwood, D. L.; Russel, D. H. *Anal. Chem.* **1990**, *62*, 268R.
(7) Stuke, M. *Appl. Phys. Lett.* **1984**, *45*, 1175−7.
(8) Brophy, J. H.; Rettner, C. T. *Opt. Lett.* **1979**, *4*, 337−9.
(9) Voigtman, E.; Jurgensen, A.; Winefordner, J. D. *Anal. Chem.* **1981**, *53*, 1921−3. Voigtman, E.; Winefordner, J. D. *Anal. Chem.* **1982**, *54*, 1834−9.
(10) Yamada, S.; Hino, K.; Kano, K.; Ogawa, T. *Anal. Chem.* **1983**, *55*, 1914−7.
(11) Yamada, S. *Anal. Chem.* **1991**, *63*, 1894−97.
(12) Judge, J. W.; McGuffin, V. L. *Anal. Chem.* **1991**, *63*, 2564−70.
(13) Schechter, I.; Schröder, H.; Kompa, K. L. *Anal. Chem.* **1992**, *64*, 2787−96.
(14) Schechter, I.; Schröder, H.; Kompa, K. L. *Anal. Chem.* **1993**, *65*, 1928−31.
(15) Schechter, I.; Schröder, H.; Kompa, K. L. *Proc. SPIE-Int. Soc. Opt. Eng.* **1994**, *2092*, 186−95.
(16) Schechter, I. *Proc. SPIE-Int. Soc. Opt. Eng.* **1994**, *2366*, 21−31.
(17) Yamada, S.; Yoshida, S.; Kawazumi, H.; Nagamura, T.; Ogawa, T. *Chem. Phys. Lett.* **1985**, *122*, 391−4.
(18) Yamada S.; Ogawa T. *Anal. Chim. Acta* **1986**, *183*, 251−6.
(19) Yamada, S.; Sato, S.; Kawazumi, H.; Ogawa, T. *Anal. Chem.* **1987**, *59*, 2719−21.
(20) Yamada, S. *Anal. Chem.* **1988**, *60*, 1975−7.
(21) Nakashima, K.; Kise, M.; Ogawa, T. *Chem. Lett.* **1992**, 837−8.
(22) Kawazumi, H.; Isoda, Y.; Ogawa, T. *Chem. Lett.* **1992**, 123−4.
(23) Ogawa, T.; Kise, K.; Yasuda, T.; Kawazumi, H.; Yamada, S. *Anal. Chem.* **1992**, *64*, 1217−20.
(24) Kawazumi, H.; Isoda, Y.; Ogawa, T. *J. Phys. Chem.* **1994**, *98*, 170−3.
(25) Chen, H.; Inoue, T.; Ogawa, T. *Anal. Chem.* **1994**, *66*, 4150−3.
(26) Ogawa, T.; Sato, M.; Tachibana, M.; Ideta, K.; Inoue, T.; Nakashima, K. *Anal. Chim. Acta* **1995**, *299*, 355−60.
(27) Ogawa, T.; Yasuda, T.; Kawazumi, H. *Anal. Sci.* **1992**, *8*, 81−2.
(28) Ogawa, T.; Yasuda, T.; Kawazumi, H. *Anal. Sci.* **1992**, *64*, 2615−7.
(29) Kawazumi, H.; Yasuda, T.; Ogawa, T. *Anal. Chim. Acta* **1993**, *283*, 111−4.
(30) Sander, M. U.; Luter, K.; Troe, J. *Ber. Bunsenges. Phys. Chem.* **1993**, *97*, 953−61.
(31) Inoue, T.; Masuda, K.; Nakashima, K.; Ogawa, T. *Anal. Chem.* **1994**, *66*, 1012−4.
(32) Yamada, S. *Anal. Chem.* **1989**, *61*, 612−5.
(33) Yamada, S. *J. Photochem. Photobiol. A* **1991**, *62*, 45−52.
(34) Nakashima, K.; Kise, M.; Ogawa, T.; Kawazumi, H.; Yamada, S. *Chem. Phys. Lett.* **1994**, *231*, 81−5.
(35) Katoh, R.; Kotani, M. *Chem. Phys. Lett.* **1990**, *166*, 258−62.
(36) Zhan, Q.; Voumard, P.; Zenobi, R. *Rapid Commun. Mass Spectrom.* **1995**, *9*, 119−27.

S0003-2700(96)00323-X CCC: $12.00

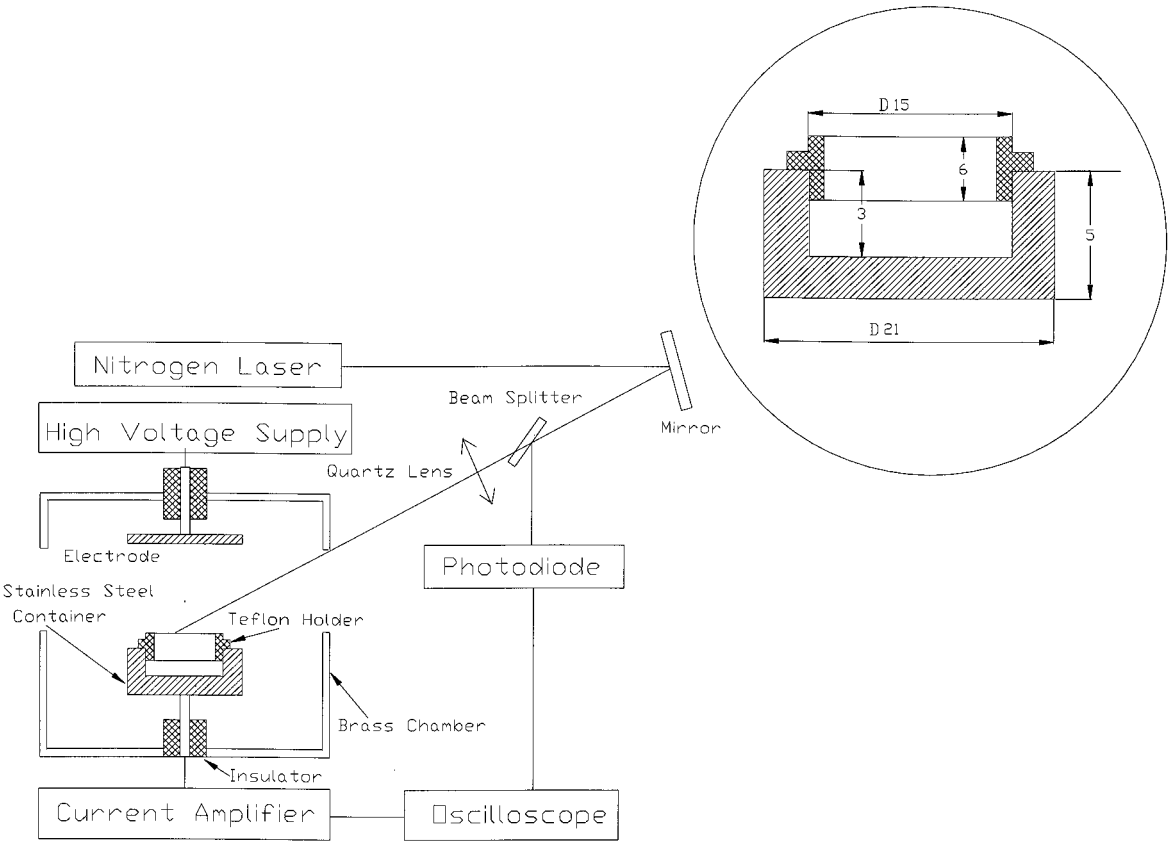

Figure 1. Schematic experimental setup.

EXPERIMENTAL SECTION

Experimental Hardware. The experimental apparatus and setup were similar to those used by Ogawa and co-workers in their conductivity study of laser multiphoton ionization of photoabsorbing molecules on a metal surface.[27,28] A schematic diagram of the experimental setup and measuring devices is shown in Figure 1. The exciting pulsed laser radiation at 337.1 nm was supplied by a nitrogen laser (PL 2300, Photon Technology International; London, Canada; 1.5 mJ in 600 ps). The laser beam was focused on the sample by a pair of cylindrical lenses and a final quartz lens ($f = 100$ mm) to a spot of $\sim$100 μm^2. Typical laser energy used was $E_{max} = 120 \pm 6$ μJ/pulse, measured slightly off focus at the sample surface. The incident angle to the samples was set at 60°. Each photoionization signal (fed from the current preamplifier) was integrated over 50 pulses by a digital oscilloscope (LeCroy 9300) triggered with a fast-responding photodiode (rise time of 20 ns). The positive voltage bias was provided by a high-voltage power supply (PS325, Stanford Research Systems, at the 2500 V/0 V on/off measurement mode). Photoionization currents, $I(t)$, were preamplified by means of a current amplifier (Keithley 428) at a typical gain level of 10^7-10^8, in the filter-off mode of the instrument. Data presented in the Results and Discussion section are given in the form that eliminates zero-bias background, i.e., for instance, $I(t) \equiv (I(t,2500\text{ V}) - I(t,0\text{ V})$.

Environmental Conditions. The photoionization study of soil samples was conducted under usual laboratory conditions, i.e., room temperature (20 ± 2 °C), ambient air pressure (750 ± 5 Torr) and composition, and ambient laboratory moisture level (65 ± 10%). The water content in the soil samples was due to moisture adsorption from air. We stress here that the stove-baked, virtually dry, soil samples are not suitable for this kind of conductivity study, because of a strong photocharge buildup that prevents proper functioning of the instruments in the current amplification stage of the measurements. On the other hand, we found that upon establishing a thermal equilibrium with the experimental surroundings (i.e., under the above-specified laboratory conditions), stable and reproducible measurements became possible. The influence of elevated water content in the soil samples on the detectability of pyrene contamination will be reported elsewhere.

Experimental Chamber. A stainless steel disk electrode was located 10 mm above the upper surface of the soil samples. The samples were held in a Teflon insert (hereafter referred as the sample holder) fixed in a stainless steel container, which also served as a negative electrode and was directly connected to the current preamplifier. A sketch of this container, together with relevant dimensions, is given in the inset of Figure 1. The main purpose of this sample holder design was to allow measurements on moist soils (see inset of Figure 1).

Materials. Pyrene-contaminated hexane was prepared from *n*-hexane (analytical grade, Frutarom Ltd., Haifa, Israel) and pyrene (99%, Aldrich), without further purification. Pyrene concentration was varied in the range of 1 ng/mL to 1 mg/mL. These solutions were deposited in two shots of 50 μL each (± 0.3 μL, by means of a 50-μL syringe, Hamilton Co.). The dry weights of the samples varied in the range 0.8−1.1 g. All relevant physical properties of the studied samples, together with their affiliation with the specific environmental and/or model source, are listed in Table 1.

Sample Preparation. The focus of this study was on detectability of pyrene contamination deposited onto soil samples,

Table 1

soil sample	weight, g	water content, mg	particle size, μm	remarks on origin
S1	1.0517	5.3	1−10	sand; Ottawa standard; Allied Chemical
S2	1.0619	12.1	5−20	sand soil from childrens' playground
S3	1.0782	9.3	1−10	chalk stone soil 10 m from organic lab
S4	1.0130	9.5	1−10	chalk stone soil 30 m from organic lab
S5	0.8917	9.6	1−5	silica, 99%; Sigma Chemical Co.

under the above-mentioned laboratory conditions. In the course of the sample preparation routine, powdered soils were gravitationally packed into the sample holder by sedimentation of the powder particles from the powder/triply deionized water muddy mixture. This was followed by a 4-h stove (at 70 ± 5 °C) and a further 1-h room temperature drying, to equilibrate the sample water content with laboratory moisture level.

The sample-moisturizing step was carried out with the sample holder fixed in its place inside the experimental chamber, at ambient conditions. At this stage, the sample was ready for external contamination with the above-specified series of pyrene/hexane solutions. The solutions were deposited onto the sample in increasing order of pyrene concentration. Contamination of sample surfaces with pyrene/hexane solutions was carried out upon removing the upper cover of the chamber and dripping the solution directly onto the sample from a ∼1-mm height above its surface. The sample was fan-dried at 50 °C for 5 min, to evaporate the hexane. This procedure resulted in stable and reproducible conductivity signals.

During photoionization measurements on any particular soil sample, the laser focus and its position on the sample surface remained unperturbed for the entire series of the pyrene/hexane solutions used.

RESULTS AND DISCUSSION

Hereafter, x refers to the concentration of contaminant; the freshly prepared uncontaminated soil samples (i.e., with $x = 0$) are referred as *virgin* samples; all relevant properties associated with *virgin* or *contaminated* samples are marked in the following by the subscript v or x, respectively.

Typical time profiles for the detected photoionization current, $I_x(t)$, (at $V = 2500$ V) are shown in Figure 2, for two of the studied samples, S2 and S5. It is noteworthy that the general features of the fast-conductivity measurements reported earlier in analysis of metallic and liquid surfaces[27−31] are readily found here too. In particular, the signals shown have a fast-response part due to conductivity by photoelectrons. This is followed by a slow-response part, which reflects a charge migration process, caused by capturing of electrons by oxygen molecules (present in ambient conditions).

The results for the lowest ($x = 0$) and the highest ($x = 1$ mg/mL) concentration of pyrene in hexane are shown in Figure 2, panels a and b, respectively. Note that despite the quite substantially different background signals from the virgin samples, the entries measured at the highest contamination levels used are essentially of the same magnitude. The same is true, in fact,

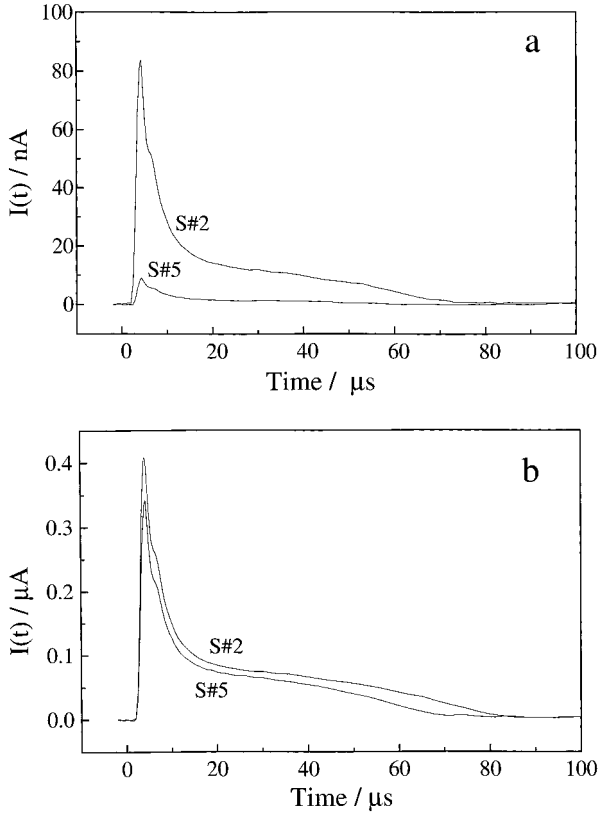

Figure 2. Photoionization current, $I = I(t)$, from two soil samples, as recorded by the digital oscilloscope. (a) $x = 0$; (b) $x = 1$ mg/mL.

for the photoionization charge, Q_x, which is represented by the area under the $I_x(t)$ curves. This suggests that for such significant contamination doses the exciting photon flux is primarily absorbed by the pyrene layer adsorbed at the sample surface and the detection ability has very little to do with the nature of the underlying substrate (soil).

Moreover, we observed that the signals detected from the studied virgin soils were different not only in the integrated charge released but also in the effective order of the photoionization process. In the kth order of an off-resonance photoionization process, obtained by means of a monochromatic photon flux of intensity Φ, with a single electron released per any successful ionization event, the detected photocharge, Q, is related to Φ as $Q \sim \Phi^k$. Hence, the slope of the log−log plot of Q versus the incoming laser beam intensity, $E(\Phi \sim E)$, should produce the effective (i.e., statistical mean value) order of the photoionization process involved.

The log−log plot of the photoionization charge versus laser intensity is illustrated in Figure 3. Here, Q_v is shown as a function of E, for all virgin samples ($x = 0$). For clarity reasons, the data are presented in a normalized form, Q/Q^*, such that $Q = Q_v$ and $Q^* = Q_v^*$; [$Q_v^* \equiv Q_v$ ($E_{max} \equiv E^*$)]. The values of Q_v^* for each sample are provided in Table 2. This table also provides the reproducibility (obtained in repeated measurements on the studied samples). It is expressed in percentage of the specified figure in this table.

One observes that the synthetic soils, samples S1 and S5, have shown a four-photon ionization process. Most likely this is due to the ionization of the water adsorbed from air onto the sample particles. The environmental samples, S3 and S4, collected near an organic chemistry laboratory, indicate a nearly two-photon

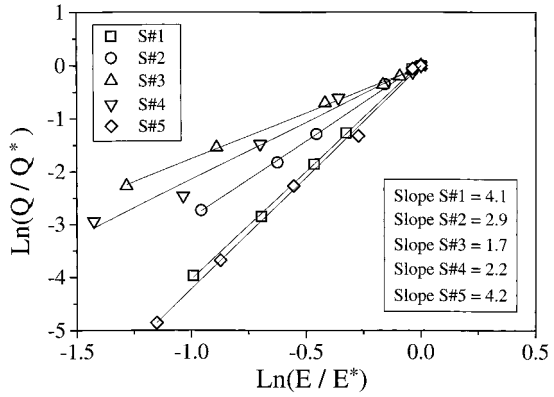

Figure 3. Normalized photoionization charge versus laser intensity; $x = 0$. Note the variety of slopes (= ionization orders), that characterize the samples.

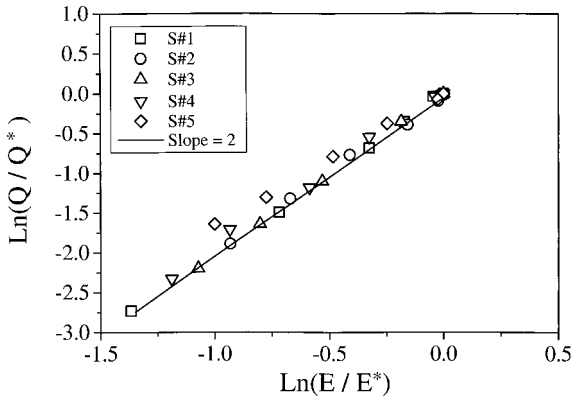

Figure 4. Normalized photoionization charge versus laser intensity; $x = 1$ mg/mL. The global ionization order of 2 indicates pyrene coverage saturation.

Table 2

soil sample	Q_v*/100fC (±8%) $x = 0$ mg/mL	Q_x*/100fC (±2%) $x = 1$, mg/mL
S1	7.9	61.9
S2	14.7	75.0
S3	2.6	63.0
S4	13.2	89.3
S5	1.5	59.3

process. This ionization order is expected for many organic compounds irradiated by photon energy of ~3.7 eV, as emitted by our N_2 laser. Nevertheless, the other environmental sample, S2, indicates a three-photon process ($k \cong 3$). This illustrates that, even for soils that are quite rich in organic components, the effective order, k, could differ from 2.

Thus, on its own, the order of the photoionization process could not be used as the sole indicator of possible present contamination, nor as a clear-cut indicator of their nature. Since the method used here is essentially a surface probe, one should be careful in drawing overreaching conclusions about the bulk properties of the investigated soils.

To further emphasize this point, we show in Figure 4 that upon external contamination of our soils with pyrene/hexane solutions at the highest concentration ($x = 1$ mg/mL), the observed order of the major contribution to the photoionization signals was $k \cong 2$ for all samples. This is due to the large (saturated) surface concentration of pyrene, which possesses a two-photon ionization at the laser wavelength (337.1 nm). The data presentation in this figure is similar to the one used for Figure 3; here $Q = Q_x - Q_v$ and $Q^* = Q_x^* - Q_v^*$. The corresponding Q_x^* values for this case are also found in Table 2. It is noteworthy that a selective trace detectability of organic contamination should be possible when variation of laser wavelength allows discrimination of the off-resonance multiphoton ionization process relative to their resonance counterparts. The same conclusion has been drawn in studies on metallic surfaces and on nonpolar solvents.[31]

In the following we describe an observation made in this study that indicates a possible compensation for matrix effects in soil analysis using the MPI method. Let $Q_S(x)$ denote the photoionization charge detected for a particular soil sample (such that S = S1, ..., S5) at a concentration x of pyrene in the deposited solution. $Q_S(0)$ then is the background signal for that sample. [Note that, in each particular case, $Q_x^* \equiv Q_S(x = 1$ mg/mL) and $Q_v^* \equiv Q_S(0)$, for that sample.]

It is clear from the above findings that the photoionization order, k, for the background signal could be quite different from the photoionization order due to adsorbed pyrene contamination. With a fixed incoming photon flux and letting the x-dependent quantum yield of the photoionization event involving pyrene molecules only, $G(x)$, to be sample independent we write for $Q_S(x)$

$$Q_S(x) = Q_S(0) + A_S G(x) \tag{1}$$

where A_S stands for the sample-dependent geometrical characteristics, which correspond to the pyrene-adsorbing ability of each particular soil under the contamination procedure used here. More explicitly, $G(x)$ contains such factors as Γ_k, the quantum-mechanical cross section for the photoionization event of order k ($k = 2$ for pyrene at 337.1 nm); Φ^k, the photon flux density; and $n(x)$, the x-dependent number of neutral pyrene molecules available for excitation by incoming photons. Additionally, $G(x)$ is inherently dependent on the interaction time, τ_k, and volume, V_k, via an implicit factor, $f(\tau_k, V_k)$.

The factor A_S could be regarded as a geometrical cross section for adsorbing pyrene onto the soil particles. Therefore, with $G(x) \sim \Gamma_k \Phi^k n(x)\, f(\tau_k, V_k)$, the above suggested eq 1 could be used to eliminate all the sample-dependent quantities by forming $\Psi(x) \equiv (F/F^*$, with $F = F(x) \equiv Q_S(x) - Q_S(0)$, $F^* = F(x^*)$ and $x^* = x_{max} = 1$ mg/mL.

In fact, any x-value from the experimental range could be used as a fixed point. This choice does not affect the main result and only produces a different scaling factor. Here, the entries of Table 2 are chosen for such a construction. Hence, thus defined $\Psi(x)$ results in

$$\Psi(x) = n(x)/n(x^*) \tag{2}$$

and represents a *sample-independent* property of the pyrene deposition process modeled in our study.

Figure 5 presents a log−log plot of $\Psi = \Psi(x)$ for the studied samples. The sample-independent nature of the resulting curve is self-evident. The straight line in this figure has a slope of 1 and corresponds to the situation for which the number of neutral pyrene molecules contributing to the detected photoionization charge is a linear function of the concentration of the deposited pyrene/hexane solution.

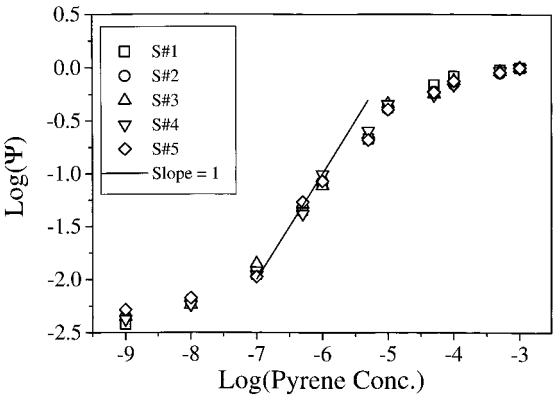

Figure 5. Plot of $\Psi = \Psi(x)$, for all examined soils. The overlapped plots, over 6 orders of concentration, indicate that geometrical and matrix effects have been eliminated.

The above plot can be used to obtain an upper (somewhat conservative) estimate of pyrene LOD in these measurements: For this purpose we consider only the linear range of the plot, which starts at ~100 ng/mL. This figure, taking a typical soil density of ~2.9 g/mL, corresponds to 35 ng/g.

It is quite clear that $n(x)$ is subject to the restrictions imposed by the extent of the interaction volume for the photoionization events inside the focused laser spot. The subsequent replacement of the active surface contamination by further deposition of pyrene/hexane solutions of ever increasing concentrations should, therefore, have a tendency to reach saturation values. This is evident for $x > 10$ μg/mL, in Figure 5. Saturation starts after the inflection region marked by a solid line of slope 1 is passed. In principle, had we studied pyrene contamination of solid (i.e., impermeable) surfaces, one could also expect that a linear dependence region of $n = n(x)$ would be followed by a saturation-like trend for high x-values. Since pyrene/hexane solution permeates into the soil sample for as long as the hexane has not evaporated, this gives a qualitative explanation for the functional dependence of $n(x)$ found here. In particular, the migration of pyrene into the soil is responsible for shape of the plot at low values of x in Figure 5 (i.e., $x < 100$ ng/mL) and for the existence of the inflection region.

(37) Pace, C. M.; Betowski, L. D. *J. Am. Soc. Mass Spectrom.* **1995**, *6*, 597−607.
(38) Lipniak, M.; Zastepa, P.; Gawlik, M. *Rocz. Panstw. Zakl. Hig.* **1994**, *45*, 97−106.
(39) Pathirana, S.; Connell, D. W.; Vowles, P. D. *Ecotoxicol. Environ. Sci.* **1994**, *28*, 256−69.
(40) Wetzel, A.; Werner, D. *Environ. Toxicol. Water Qual.* **1995**, *10*, 127−33.
(41) Kirso, U.; Tanner, R.; Irha, N. *Eesti Tead. Akad. Toim. Keem.* **1995**, *44*, 13−20.

CONCLUSIONS

The MPI process, coupled with a fast photocurrent detection system, has been used for the study of pyrene-contaminated soils. This method can handle contamination a wide dynamic range (6 orders of magnitude) and a variety of initial soils. According to our estimate, pyrene detection limit is below 35 ng/g, which is adequate for environmental soil analysis. Target PAH concentrations in contaminated soils are in the range of 0.85−125 μg/g.[37−41]

Although the ionization order in initial samples varies between 2 and 4, the additional pyrene contamination could be monitored.

Moreover, by assuming a contamination model that separates geometrical effects from the pure MPI process, a remarkable compensation for matrix effects has been carried out. This model of an external contamination where impurities are deposited onto the soil surface by contaminated solvents suggests that the detection ability of the applied method could be influenced by the permeability of the soil surface with respect to the solvent. This result brings about several directions for further studies on this subject: For example, the investigation of aerosol-type depositions, where the soil is heavily watered and neither the solvent nor the impurity is readily mixed or dissolved in the water table of the soil, is of current environmental interest. When the contamination is brought to the soil surface from below, by means of capillary effects, the method could help to relate, in a nondestructive manner, the surface concentrations with the internally present ones.

This study points out the feasibility of soil analysis by the proposed method; however, there are still several effects (e.g., moisture dependence) to be understood before commercial applications are possible. These effects are now under investigation.

ACKNOWLEDGMENT

This research was supported, in part, by the James-Franck Program for Laser Matter Interaction and by the VPR Fund, Technion-IIT. V.V.G. and V.B. are grateful for partial financial support provided by the Israeli Ministry of Science and Technology and by the Ministry of Absorbtion to the scientists regarded as return citizens and/or new immigrants.

Received for review April 2, 1996. Accepted June 15, 1996.[⊗]

AC9603237

[⊗] Abstract published in *Advance ACS Abstracts,* August 1, 1996.